



HAL
open science

Mapping the geometry of volcanic systems with magnetotelluric soundings: results from a land and marine magnetotelluric survey performed during the 2018-2019 Mayotte seismovolcanic crisis

Mathieu Darnet, Pierre Wawrzyniak, Pascal Tarits, Sophie Hautot,
Jean-François d'Eu

► **To cite this version:**

Mathieu Darnet, Pierre Wawrzyniak, Pascal Tarits, Sophie Hautot, Jean-François d'Eu. Mapping the geometry of volcanic systems with magnetotelluric soundings: results from a land and marine magnetotelluric survey performed during the 2018-2019 Mayotte seismovolcanic crisis. 25th EM Induction Workshop, Sep 2022, Çeşme, Turkey. hal-03693765

HAL Id: hal-03693765

<https://brgm.hal.science/hal-03693765>

Submitted on 13 Jun 2022

HAL is a multi-disciplinary open access archive for the deposit and dissemination of scientific research documents, whether they are published or not. The documents may come from teaching and research institutions in France or abroad, or from public or private research centers.

L'archive ouverte pluridisciplinaire **HAL**, est destinée au dépôt et à la diffusion de documents scientifiques de niveau recherche, publiés ou non, émanant des établissements d'enseignement et de recherche français ou étrangers, des laboratoires publics ou privés.

Mapping the geometry of volcanic systems with magnetotelluric soundings: results from a land and marine magnetotelluric survey performed during the 2018-2019 Mayotte seismovolcanic crisis

Mathieu Darnet¹, Pierre Wawrzyniak¹, Pascal Tarits², Sophie Hautot³ and Jean-François D'eu⁴

¹BRGM – French Geological Survey, Orléans, France – m.darnet@brgm.fr or p.wawrzyniak@brgm.fr

²IUEM, Institut Universitaire Européen de la Mer, LGO, UMR 6538 - IUEM/UBO - pascal.tarits@univ-brest.fr

³IMAGIR Sarl, Saint Renan, France - sophie.hautot@imagir.eu

⁴MAPPEM Geophysics SAS, Saint Renan, France - jf.deu@mappem-geophysics.com

SUMMARY

A major seismovolcanic crisis has afflicted the islands of Mayotte, Comoros Archipelago, since May 2018, although the origin is debated. Magnetotellurics (MT), which is sensitive to hydrothermal and/or magmatic fluids and can map the subsurface electrical resistivity structure, can provide insight by revealing the internal structure of the volcanic system. In this paper, we report the results of a preliminary land and shallow marine MT survey performed on and offshore the island nearest the crisis. The 3D inversion-derived electrical resistivity model suggests that the island is underlain by a shallow ~500-m-thick conductive layer atop a deeper, more resistive layer, possibly associated with a high-temperature geothermal system. At depths of ~15 km, the resistivity drops by almost two orders of magnitude, possibly due to partial melting. Further petrophysical and geophysical studies are underway for confirmation and to map the geometry and evolution of the volcanic system.

Keywords: magnetotelluric, electrical resistivity, seismovolcanic, geothermal

INTRODUCTION

Mayotte, located along a WNW-ESE oceanic ridge at the boundary of the Lwandle and Somalian plates, represents a region of islands within the volcanic Comoros Archipelago north of the Mozambique Channel between the northern tip of Madagascar and the eastern coast of Mozambique. The region of Mayotte is composed predominantly of two main islands, namely, Grande Terre (363 km²) to the west and Petite Terre (11 km²) to the east (figure 1).

In May 2018, an offshore seismovolcanic crisis initiated approximately 50 km to the east of Mayotte; the crisis included the largest seismic event ever recorded in the Comoros with a Mw=5.9 and an estimated 5 km³ of lava was released from an eruptive site in the same area (REVOSIMA bulletin, <http://www.ipgp.fr/fr/actualites-reseau>).

The seismicity subsequently migrated to the west and is now located between 5 and 15 km from the Petite Terre. The possible causes of the Comoros volcanism continue to constitute a topic of controversy (Lemoine et al., 2019), as its origin could be related to i) the presence of a hot spot, ii) lithospheric fractures, or iii) a combination of the two, i.e., regional extension in conjunction with asthenospheric processes. Forecasts regarding the evolution of this crisis remain very uncertain and require the gathering of additional geoscientific data,

particularly geophysical data, to help understand the internal structure of the corresponding volcanic system.

In this paper, we present the results of an land and shallow marine Magneto-Telluric (MT) survey carried out during the seismovolcanic crisis of Mayotte.

MT DATA ACQUISITION AND PROCESSING

Due to its high degree of urbanization, Petite Terre island presents a challenging environment in which to perform passive electromagnetic (EM) measurements. To mitigate the impacts of ambient EM noise on the MT soundings, we deployed two MT stations on the most isolated parts of the island (sites L1 and L2) and one remote reference MT station on Grande Terre island (site L0), approximately 15 km away from Petite Terre (figure 1). We used ADU07 systems (Metronix, Germany) with unpolarizable Pb-PbCl₂ electrodes (Wolf Ltd, Hungary) and MSF07 magnetic coils (Metronix, Germany). The sensors were oriented toward the north and east (x=north, y=east). MT recordings were performed synchronously for 4 days at both sites.

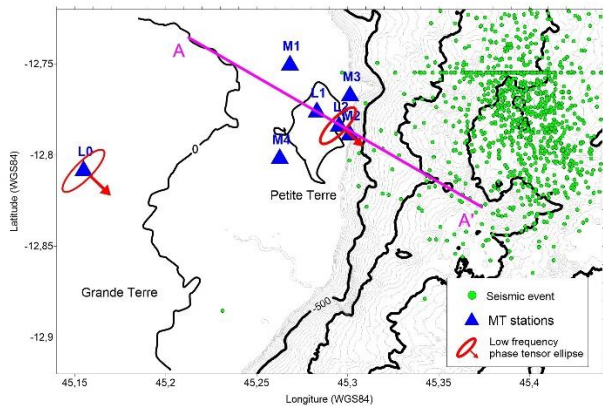


Figure 1. Location of the MT stations deployed onshore and offshore Petite Terre island. The blue triangles represent the MT sites. The green circles represent the epicenters of the seismic events recorded from May 2018 to May 2019. The red ellipses with an arrow represent the phase tensor ellipses at 1000 s at sites L0 and L2. Profile AA' is the location of the cross-section through the 3D resistivity model in Figure 3.

We processed the time series following the robust approach of Chave and Thomson. (2004) with a remote reference MT station. We computed the full impedance tensor at each site at periods ranging from 0.001 to 1000 s. An MT sounding example is shown in figure 2. Overall, the data were of good quality over the period range; however, at 1-10 s, noise could not be excluded due to the weakness of the primary field. The phase tensor ellipses shown in figure 1 were extracted from the phase tensors calculated using the formula of Booker (2014).

Because of the limited number of sites favorable for MT measurements on Petite Terre island, we deployed four new-generation low-power shallow marine MT systems (STATEM) around the island at water depths ranging from 15 to 25 m (figure 1). These STATEM systems were recently developed by MAPPEM Geophysics and the Ocean Geosciences Laboratory (LGO), European Institute for Marine Studies (IUEM). Each STATEM system records the two horizontal components of the electric field with 5m-long electric dipoles and marine Ag-AgCl electrodes. The three components of the magnetic field were obtained from a 3-component fluxgate sensor. With an optimized datalogger, the measurements were performed synchronously with the land stations for 2 days at a sampling rate of 512 Hz. The design of the system is such that motion of the system induced by oceanic current is minimized. During the survey, bidirectional tiltmeter measurements performed every second showed that motion and drift of the sensor were minimum (less than +/- 0.2 deg).

Similarly to the land case, the time series were robustly processed with the bounded influence, remote reference processing (BIRRP). The processing of shallow marine MT data is a challenging task due to the high level of ocean-induced EM noise that can mask the MT signal. For the electric field, noise can be generated not only by the movement of the water layer (e.g., waves, swells, tides) within the Earth's magnetic field but also by the current-induced motion of the electrodes. Similarly, magnetic field measurements can become contaminated by noise associated with not only ocean-induced electric currents but also the motion of the sensor. As a consequence, both electric and magnetic measurements may exhibit high levels of ocean-induced EM noise that is well correlated and difficult to distinguish from the MT signal. Therefore, the use of a land remote reference is of paramount importance to reduce the impacts of ocean-induced noise. Remote referencing between marine sites was sufficient at long periods (>100 s); hence, the challenge was to obtain the MT impedance at the shortest possible period (<0.1 s). Depending on the type of noise, magnetic and/or electric field measurements from the remote reference were used to filter out oceanic noise. An example of the MT transfer function is shown in figure 2. Despite the lack of high-frequency measurements (<0.01 s) due to the weakness of the MT signals recorded beneath ~20 m of seawater, the MT transfer function was reliably recovered over the 0.02 - 1000 s period band and was consistent with the nearby land site (site L2). Nevertheless, similar to the land data, the MT impedance results at 1-10 s were not reliable, as this period range is further impacted by a high level of swell-induced noise.

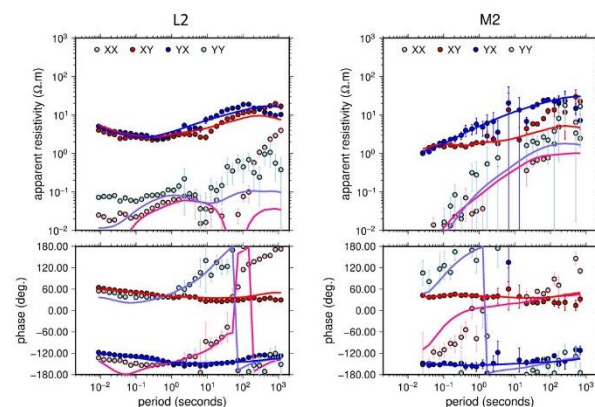


Figure 2. MT soundings for sites L2 (left panel) and M2 (right panel). The upper and lower panels display the apparent resistivity in Ohm.m and phase in degrees, respectively. The full lines signify the responses of the best-fitting model.

MT INVERSION RESULTS

The data recorded at the two land and the four marine MT sites were jointly inverted to image the electrical resistivity structure beneath Petite Terre island. We inverted the four components of the MT impedance tensors at all available periods; the period range for the land MT data was 0.009-1000 s, and that for the marine MT data was 0.02-1000 s. We excluded data with large errors, especially within the dead band. For the 3D inversion, we used the MININ3D code from Hautot *et al.* (2007). Given the small number of sites, we used a grid of 21x18x18 cells, which included the bathymetry of the study area. The total volume of the 3D model was 21x20x13 km³. The horizontal dimensions of the cells in the central part of the model is 500 x 500 m. The thickness of the layers increased from 5 to 5000 m. The 3D model topped a 1D model with three layers with thicknesses of 13, 38 and 88 km, whose resistivities were also included in the inversion. Except for the marine part (0.3 Ohm.m), the starting model was homogeneous (18 Ohm.m). The 3D inversion was applied to minimize a misfit function between the observed data and the 3D model response at all sites and frequencies weighted by the data variance. Data were the four complex components of the MT tensor. The starting RMS was 9.3, and the RMS decreased down to 2.2.

A cross-section through the shallow (until 5km depth) and deep (until 50km depth) section of the 3D resistivity model is shown in figure S2 and figure 3, respectively. The most prominent feature is the presence of a deep conductive layer (with a resistivity of less than 2 Ohm.m) beneath a depth of 13 km (labelled C1 on figure 3). A shallow conductive layer (resistivity of less than 5 Ohm.m) is also present within the first 500 m of the model (labelled C3 on figure S2). Between these two conductive structures, the resistivity increases up to ~100 Ohm.m. Toward the southeast, the resistivity in the 5-13 km depth range decreases to less than 10 Ohm.m (labelled C2 on figure 3); this conductor is located close to the hypocenters of the seismic events recorded during the seismovolcanic crisis.

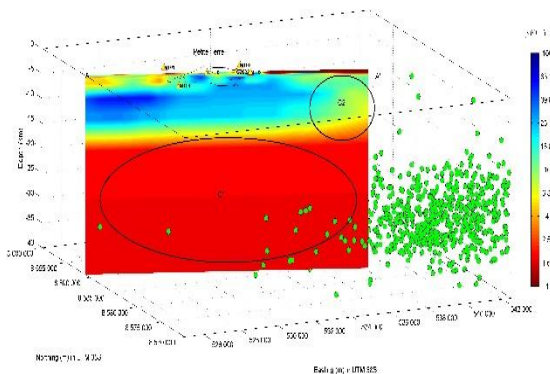


Figure 3. N120° cross-section through the 3D resistivity volume obtained from the inversion of the land and marine MT data. Green circles represent the hypocenters of the seismic events recorded from May 1, 2018, to May 28, 2019 (Lemoine 2019 volcano). Yellow triangles represent the MT sites used in the MT inversion.

To assess the uncertainties in the deep resistivity structures identified in the 3D resistivity model, we performed a sensitivity analysis on both the resistivity of the conductive layer (below a depth of 13 km) and the depth to the top of this conductor (figure 4). The misfit rapidly increases with increasing resistivity below a depth of 13 km, confirming that a conductor of less than 4 Ohm.m is required to fit the data (figure 4a). The optimum depth of this conductor was found at approximately 16 km (figure 4b). However, the misfit increases slowly between this interval indicating that this depth is not very well resolved. We also tested the sensitivity of the model to the presence of the C2 conductor between depths of 5 and 13 km to the southeast of Petite Terre and on the edge of the MT network (figure 3). The absence of this conductor significantly increased the misfit (figure 4c), suggesting that this feature was not an artifact of the inversion process and was constrained by the MT data.

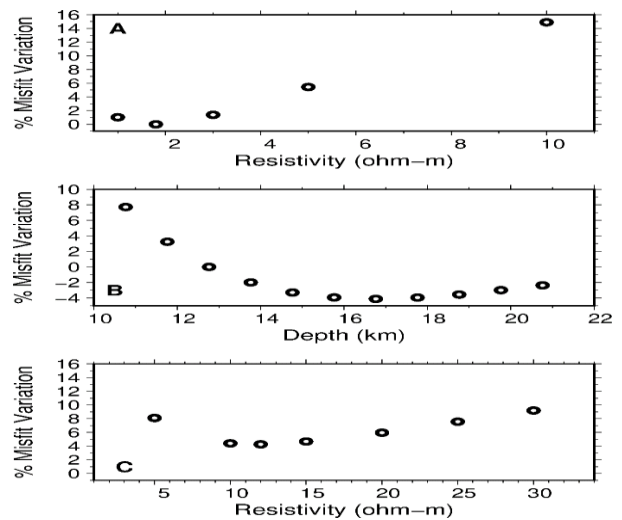


Figure 4. Variation of the misfit between the tested and preferred model as a function of a) the resistivity of the deep conductive layer, b) the depth of the top of this conductor and c) the presence of a conductor between 5 and 13km depth to the South-East of Petite Terre. The value 0 corresponds to the preferred model.

DISCUSSION

The presence of a shallow conductive layer overlying a more resistive body beneath the surface

of Petite Terre (labelled C3 in figure 3) is consistent with the electrical resistivity structure typically observed under volcanoes exhibiting well-developed hydrothermal systems (Flovenz *et al.*, 2005). According to these models, this shallow conductive layer (resistivity of 1-10 Ohm.m) corresponds to a smectite-rich, low-temperature (<220°C), hydrothermally altered layer, often called a clay cap. For Petite Terre, this layer would be approximately 500 m thick. At greater depth and with increasing temperature (>220° C), the material is less rich in smectite, whereas the illite content increases. Furthermore, porosity tends to decrease with depth, which reinforces the modeled resistivity increase due to the change in alteration products with resistivity values ranging from 20 to 100 Ohm.m. On Petite Terre, such values are observed below depths of 500 m and deeper and could correspond to a high-temperature geothermal reservoir.

At depths of 13-16 km, the resistivity drops by almost two orders of magnitude, reaching values of a few Ohm-meters (labelled C1 on figure 3). These low resistivities could be caused either by the presence of altered rocks saturated with fluid below the supercritical point (<400°C) or by the presence of a small fraction of connected melt. At these depths, the temperature exceeds the supercritical point; hence, the most likely explanation for the observed conductive layer is the presence of melt. Similar observations have been reported beneath oceanic ridges on the basis of MT soundings (Baba, 2006) and interpreted as being indicative of the presence of melt (Laumonier *et al.*, 2017). Nevertheless, additional laboratory data (e.g., electrical resistivity measurements on Mayotte volcanic rock samples) and geophysical observations (e.g., seismic tomography) are necessary to confirm this interpretation.

Finally, we noticed the presence of a conductive structure in the 5-15 km depth range to the southeast of Petite Terre (labelled C2 on figure 3) close to the seismic events recorded between May 2018 and May 2019. In this area, recent volcanic material and gas emissions have been observed on the seafloor. Accordingly, this conductive anomaly could be related to recent seismovolcanic activity. Additional deep marine MT sites are currently being deployed in this area to obtain more insight into the presence and geometry of this conductive anomaly and its relationship with the regional seismovolcanic activity. Furthermore, the land stations at sites L0 and L2 are currently being monitored continuously to perform robust-processing of the deep marine MT sites but also long-term monitoring of any resistivity changes at depth related to the evolution of the seismovolcanic crisis.

CONCLUSIONS

Since May 2018, a major seismovolcanic crisis has affected the islands of Mayotte in the Comoros Archipelago, providing a unique opportunity to monitor the development of an active volcanic system. Preliminary MT data acquired on and near this island were implemented to image the electrical resistivity structure of the volcanic system. The resulting model suggests the presence of hydrothermal fluids in the shallow part of the system (< 2 km) and magmatic fluids at greater depth (> 15 km). Further petrophysical and geophysical studies (e.g. additional land and offshore MT surveys, seismic surveys) are ongoing to confirm the origin and geometry of these deep conductors and to help better understand the associated magmatic and volcanic activity.

ACKNOWLEDGEMENTS

We would like to thank the General Directorate for Risk Prevention (DGPR) for financially supporting the geophysical work.

REFERENCES

- Baba, K., Chave, A.D., Evans, R.L., Hirth, G., Mackie, R.L., 2006. Mantle dynamics beneath the east pacific rise at 17 s: Insights from the mantle electromagnetic and tomography (melt) experiment. *Journal of Geophysical Research: Solid Earth* 111.
- Booker, J.R., 2014. The magnetotelluric phase tensor: a critical review. *Surv. Geophys.* 35, 7–40.
- Chave, A.D., Thomson, D.J., 2004. Bounded influence magnetotelluric response function estimation. *Geophys. J. Int.* 157, 988–1006.
- Flóvenz, Ó., Spangenberg, E., Kulenkampff, J., Árnason, K., Karlsdóttir, R., Huenges E., 2005. The role of electrical interface conduction in geothermal exploration. In: *Proceedings of the 2005 World Geothermal Congress*. pp. 24–29.
- Hautot, S., Single, R., Watson, J., Harrop, N., Jerram, D., Tarits, P., Whaler, K., Dawes, D., 2007. 3-d magnetotelluric inversion and model validation with gravity data for the investigation of flood basalts and associated volcanic rifted margins. *Geophys. J. Int.* 170, 1418–1430.
- Lemoine, A., Bertil, D., Roullé, A., Briole, P., 2019. The Volcano-Tectonic Crisis of 2018 East of Mayotte, Comoros Islands
- Laumonier, M., Farla, R., Frost, D.J., Katsura, T., Marquardt, K., Bouvier, A.S., Baumgartner, L.P., 2017. Experimental determination of melt interconnectivity and electrical conductivity in the upper mantle. *Earth Planet. Sci. Lett.* 463, 286–297.